

## Supporting Information

# Heterogeneous Hydrogenation of Phenylalkynes with Parahydrogen: Hyperpolarization, Reaction Selectivity, and Kinetics

*Ekaterina V. Pokochueva<sup>a,b</sup>, Kirill V. Kovtunov<sup>a,b,\*</sup>, Oleg G. Salnikov<sup>a,b</sup>, Max E. Gemeinhardt<sup>c</sup>,  
Larisa M. Kovtunova<sup>d,b</sup>, Valerii I. Bukhtiyarov<sup>d</sup>, Eduard Y. Chekmenev<sup>e,f</sup>, Boyd M. Goodson<sup>c,g,\*</sup>,  
Igor V. Koptug<sup>a,b</sup>*

<sup>a</sup>International Tomography Center, SB RAS, 3A Institutskaya St., 630090 Novosibirsk, Russia

<sup>b</sup>Novosibirsk State University, 1 Pirogova St., 630090 Novosibirsk, Russia

<sup>c</sup>Department of Chemistry and Biochemistry, Southern Illinois University, Carbondale, IL 62901, United States

<sup>d</sup>Boriskov Institute of Catalysis SB RAS 5 Acad. Lavrentiev Pr., 630090 Novosibirsk, Russia

<sup>e</sup>Department of Chemistry, Integrative Biosciences (Ibio), Wayne State University, Karmanos Cancer Institute (KCI), Detroit, Michigan 48202, United States

<sup>f</sup>Russian Academy of Sciences, Leninskiy Prospekt 14, Moscow 119991, Russia

<sup>g</sup>Materials Technology Center, Southern Illinois University, Carbondale, IL 62901, United States

### 1. CATALYST PREPARATION AND CHARACTERIZATION

1.1. *Materials.* Powder TiO<sub>2</sub> (Hombifine N, S<sub>BET</sub> = 197 m<sup>2</sup>/g), 10% palladium(II) nitrate solution in 10% nitric acid (Aldrich 380040), 8% chloroplatinic acid water solution (Aldrich 262587), RhCl<sub>3</sub> hydrate (cas. 20765-48-4), IrCl<sub>4</sub> (CAS: 10025-97-5, Krastsvetmet), HCl (cas.:

7647-01-0), NaOH (cas. 1310-73-2), HNO<sub>3</sub> (cas. 7697-37-2), tetramethylammonium hydroxide 25% in water (Acros, cas:75-59-2).

1.2 *Preparation.* Nitrate solutions were used as the precursor of the metal. Preparation of rhodium and platinum nitric solutions were described in Ref. <sup>1,2</sup>.

1.2.1. *Preparation of platinum nitrate solution.* An excess of a concentrated solution of NaOH (molar ratio Pt: NaOH = 1: 10) was added to the H<sub>2</sub>PtCl<sub>6</sub> solution. The reaction mixture was heated to obtain a yellow solution. Then the solution was cooled and the pH of the reaction mixture was adjusted to 6. A precipitate of H<sub>2</sub>[Pt(OH)<sub>6</sub>] formed, which was thoroughly washed with distilled water until to complete remove of Cl<sup>-</sup> ions. The resulting H<sub>2</sub>[Pt(OH)<sub>6</sub>] was dissolved in nitric acid.

1.2.2. *Preparation of rhodium nitrate solution.* An excess of a concentrated solution of NaOH (molar ratio Rh: NaOH = 1: 8) was added to the RhCl<sub>3</sub> solution. The reaction mixture was heated to decolorize the solution. Next, HNO<sub>3</sub> was added to the resulting solution to pH~10-11. A yellow-orange precipitate of Rh(OH)<sub>3</sub> was formed. It was filtered and washed with distilled water to complete remove of Cl<sup>-</sup>. An excess of HNO<sub>3</sub> was added to freshly prepared Rh(OH)<sub>3</sub>.

1.2.3. *Pt/TiO<sub>2</sub>, Pd/TiO<sub>2</sub> catalysts preparation.* A series of supported Rh, Pt, and Pd catalysts on TiO<sub>2</sub> were prepared by wet impregnation. The TiO<sub>2</sub> powder was calcined at 500 °C for 2 h prior to use. The TiO<sub>2</sub> was impregnated with a mixture of a calculated amount of nitric acid solution containing a given metal and water for 1h at room temperature, then the solvent excess was evaporated, the raw catalysts were dried in air at 120 °C for 4 h. Calcination of the impregnated support at 400 °C in air for 3 h followed by reduction in H<sub>2</sub> flow at 330 °C for 3 h finalized the preparation procedure.

1.2.4. *Rh/TiO<sub>2</sub> catalyst preparation.* For the preparation of Rh/TiO<sub>2</sub> catalysts with 1, 5, and 10 wt% metal loading, the acidic solution of Rh(NO<sub>3</sub>)<sub>3</sub> was used. A calculated amount of Rh(NO<sub>3</sub>)<sub>3</sub> solution were evaporated to dryness and after it was diluted with water to a total volume of 1.6 ml. The 2 g of TiO<sub>2</sub> was impregnated with aqueous solutions of rhodium for 1h at room temperature. Then the solvent excess was evaporated and the formed catalysts were dried in air at 120 °C for 3 h. The next calcination of the samples were performed at 400 °C in air for 4 h with subsequent reduction of samples in H<sub>2</sub> flow at 330 °C for 3 h.

For the preparation of Rh/TiO<sub>2</sub> catalyst with large metal loading (23,2 wt%) an acidic solution of Rh(NO<sub>3</sub>)<sub>3</sub> was used. The solution of Rh(NO<sub>3</sub>)<sub>3</sub> was evaporated to dryness and afterwards

diluted with water to a total volume of 2 ml and then 5 drops of solutions tetramethylammonium were added. The 2 g of  $\text{TiO}_2$  was impregnated with aqueous solutions of rhodium for 2,5 h at room temperature. Then the solvent excess was evaporated and formed catalysts were dried in air at  $120^\circ\text{C}$  for 4 h. The next calcination of the samples was performed at  $400^\circ\text{C}$  in air for 3 h with subsequent reduction of samples in  $\text{H}_2$  flow at  $330^\circ\text{C}$  for 3 h.

1.2.5. *Ir/TiO<sub>2</sub> catalyst preparation.* A portion of  $\text{IrCl}_4$  was dissolved in an excess of hydrochloric acid. The resulting solution was evaporated to dryness and distilled water was added. Pre-dried  $\text{TiO}_2$  was impregnated with the resulting solution for one hour. Then the solvent excess was evaporated and the resulting catalysts were dried in air at  $120^\circ\text{C}$  for 4 h. The next calcination of the samples was performed at  $400^\circ\text{C}$  in air for 3 h with subsequent reduction of samples in  $\text{H}_2$  flow at  $330^\circ\text{C}$  for 3 h .

1.3. *Characterization.* The metal loadings in solution were determined by inductively coupled plasma atomic emission spectroscopy (ICP-AES; OPTIMA 4300 DV; Perkin Elmer, USA). The metal loading values in the catalysts were determined by x-ray fluorescence on an ARL PERFORM'X analyzer with an Rh anode of an x-ray tube.

$\text{CO}$  and  $\text{H}_2$  chemisorption experiments were carried out on Chem BET Pulsar TPR/TPD Analyzer (Quantachrome instruments, USA).  $\text{CO}$  chemisorption measurements were done in a following way:

1. Change Gas to Helium
2. Ramp Temp to 140 at 20 deg/min
3. Wait for 5 min
4. Change Gas to Oxygen
5. Ramp Temp to 350 at 20 deg/min
6. Wait for 30 min
7. Change Gas to Helium
8. Ramp Temp to 300 in 5 min
9. Change Gas to Hydrogen
10. Wait for 60 min
11. Change Gas to Helium
12. Wait for 10 min
13. Ramp Temp to 40 in 1 min

14. Wait for 30 min

15. Titration: 10.6%CO in He.

H<sub>2</sub> chemisorption measurements were done in a following way:

1.Change Gas to Argon

2.Ramp Temp to 140 at 20 deg/min

3.Wait for 5 min

4.Change Gas to Oxygen

5.Ramp Temp to 350 at 20 deg/min

6.Wait for 30 min

7.Change Gas to Argon

8.Ramp Temp to 300 in 5 min

9.Change Gas to Hydrogen

10.Wait for 60 min

11.Change Gas to Argon

12.Wait for 10 min

13.Ramp Temp to 40 in 1 min

14. Wait for 30 min

15. Titration: 9.6%H<sub>2</sub> in Ar.

Note that for the catalyst with 3.95% Rh content metal dispersion value, found from H<sub>2</sub> chemisorption, exceeds 100% – this effect is probably explained by existence of multiple adsorption sites, and has been described elsewhere.<sup>3,4</sup>

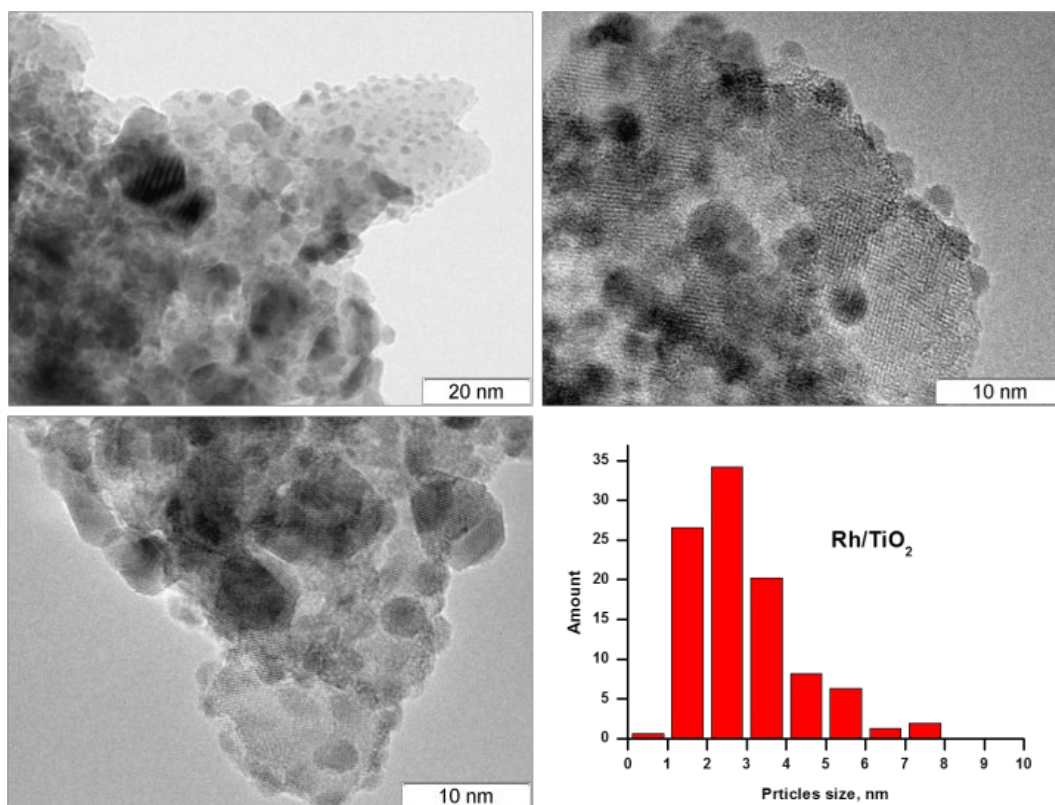


**Figure S1** - TEM images and metal particles size distribution for 23.2 wt% Rh/TiO<sub>2</sub> catalyst. The average size of metal particles is *ca.* 3 nm.

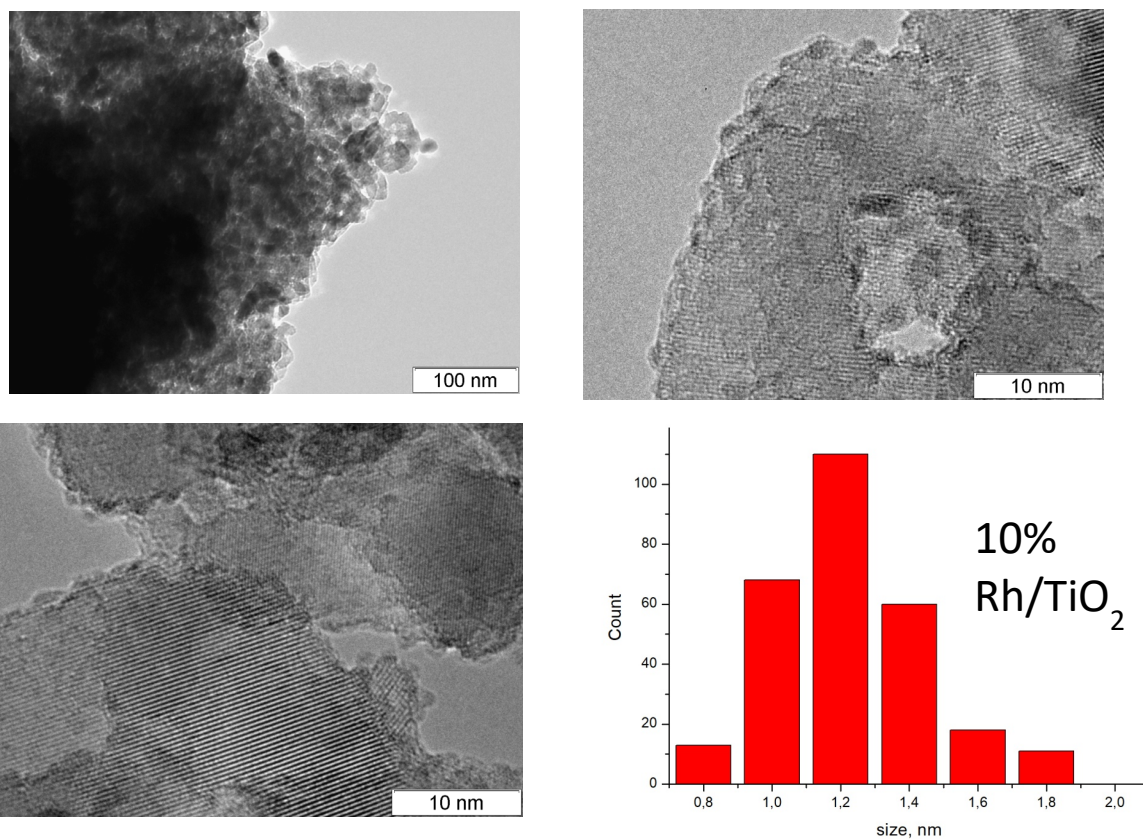


**Figure S2** - TEM images and metal particles size distribution for 10 wt% Rh/TiO<sub>2</sub> catalyst. The average size of metal particles is *ca.* 1.2 nm.

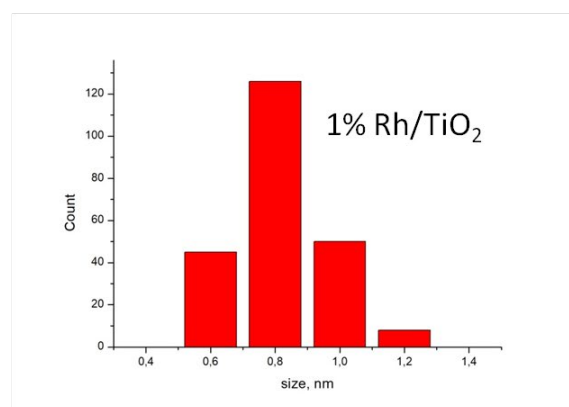
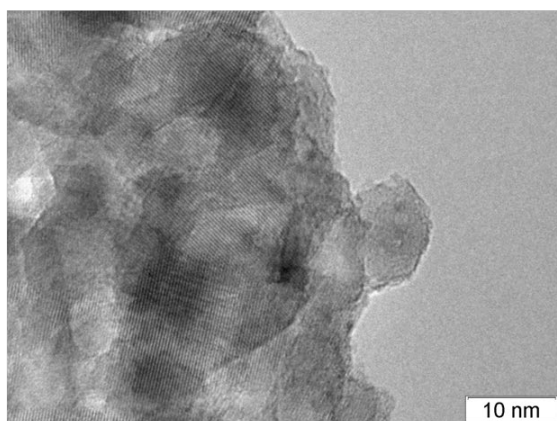
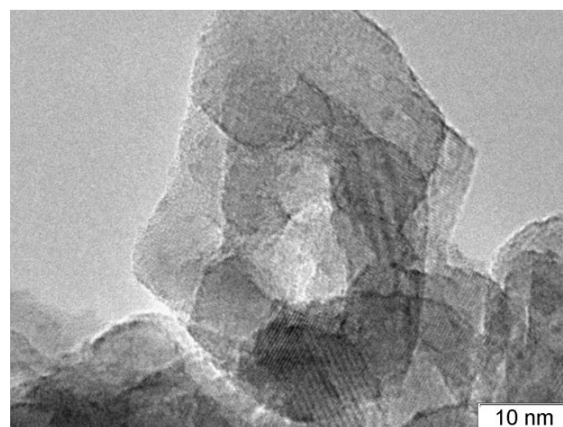
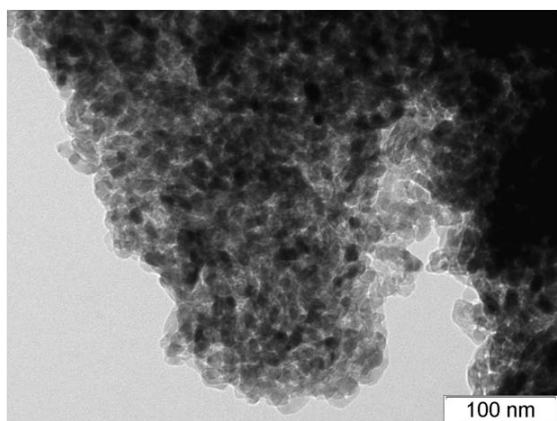


**Figure S3** - TEM images and metal particles size distribution for 1 wt% Rh/TiO<sub>2</sub> catalyst. The average size of metal particles is *ca.* 0.8 nm.

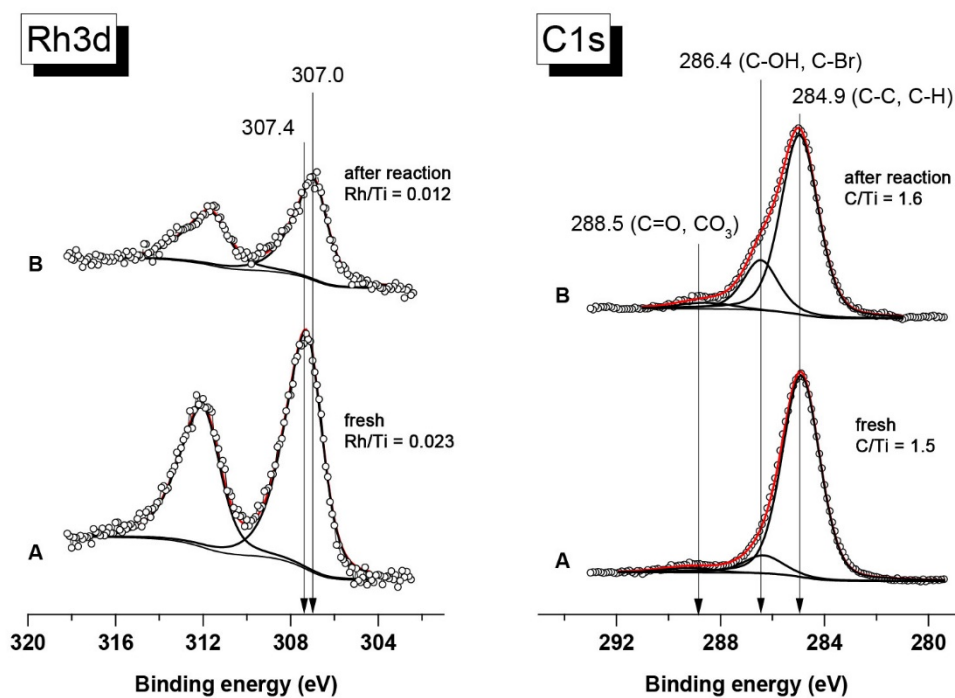


**Figure S4** - XPS spectra of Rh3d (left panel) and C1s (right panel) measured for (A) fresh Rh/TiO<sub>2</sub> and (B) Rh/TiO<sub>2</sub> after reaction.

## 2. CATALYTIC PERFORMANCE



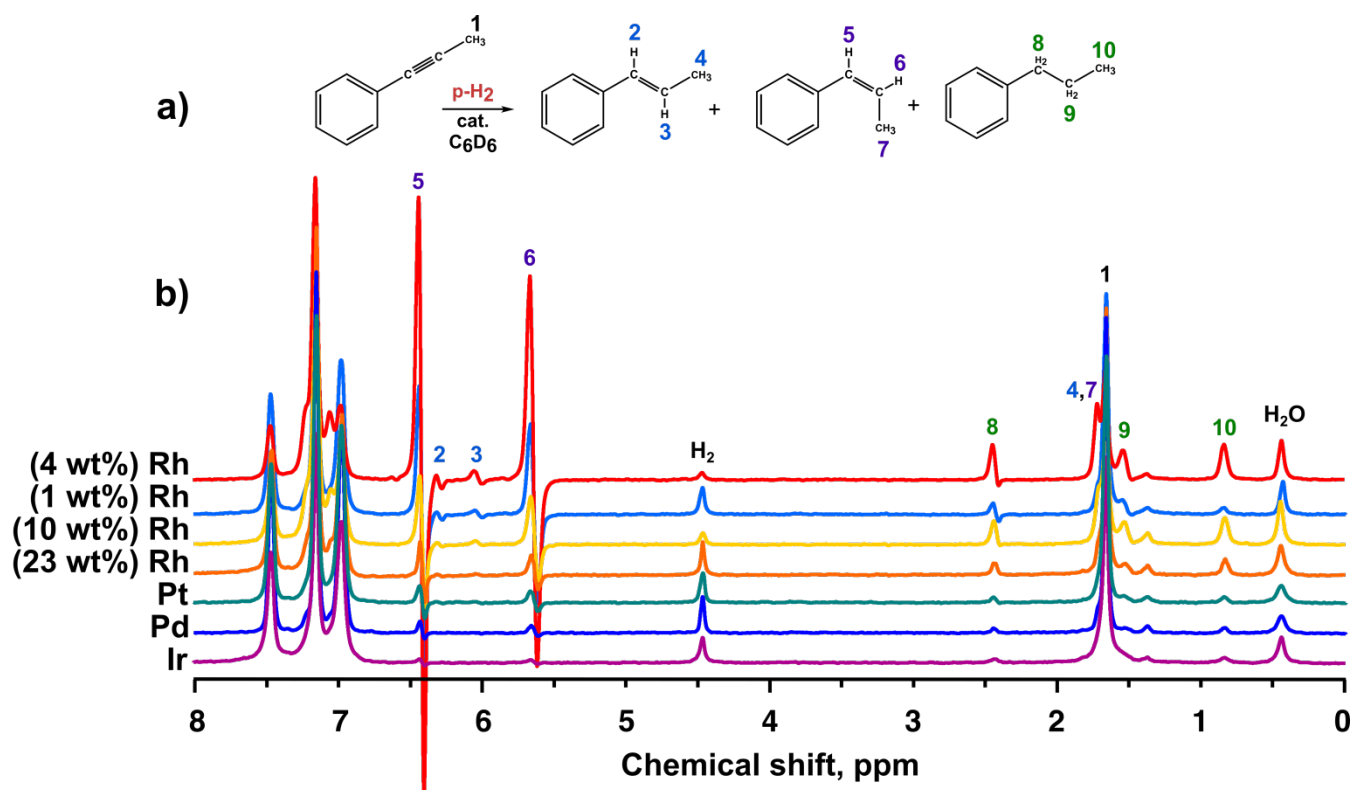


**Figure S5** - (a) Reaction scheme of 1-phenyl-1-propyne hydrogenation. (b)  $^1\text{H}$  NMR spectra acquired during hydrogenation of 1-phenyl-1-propyne with parahydrogen over different heterogeneous catalysts. Spectra are arranged (top to bottom) in descending order of polarized signal intensity (signal #5).

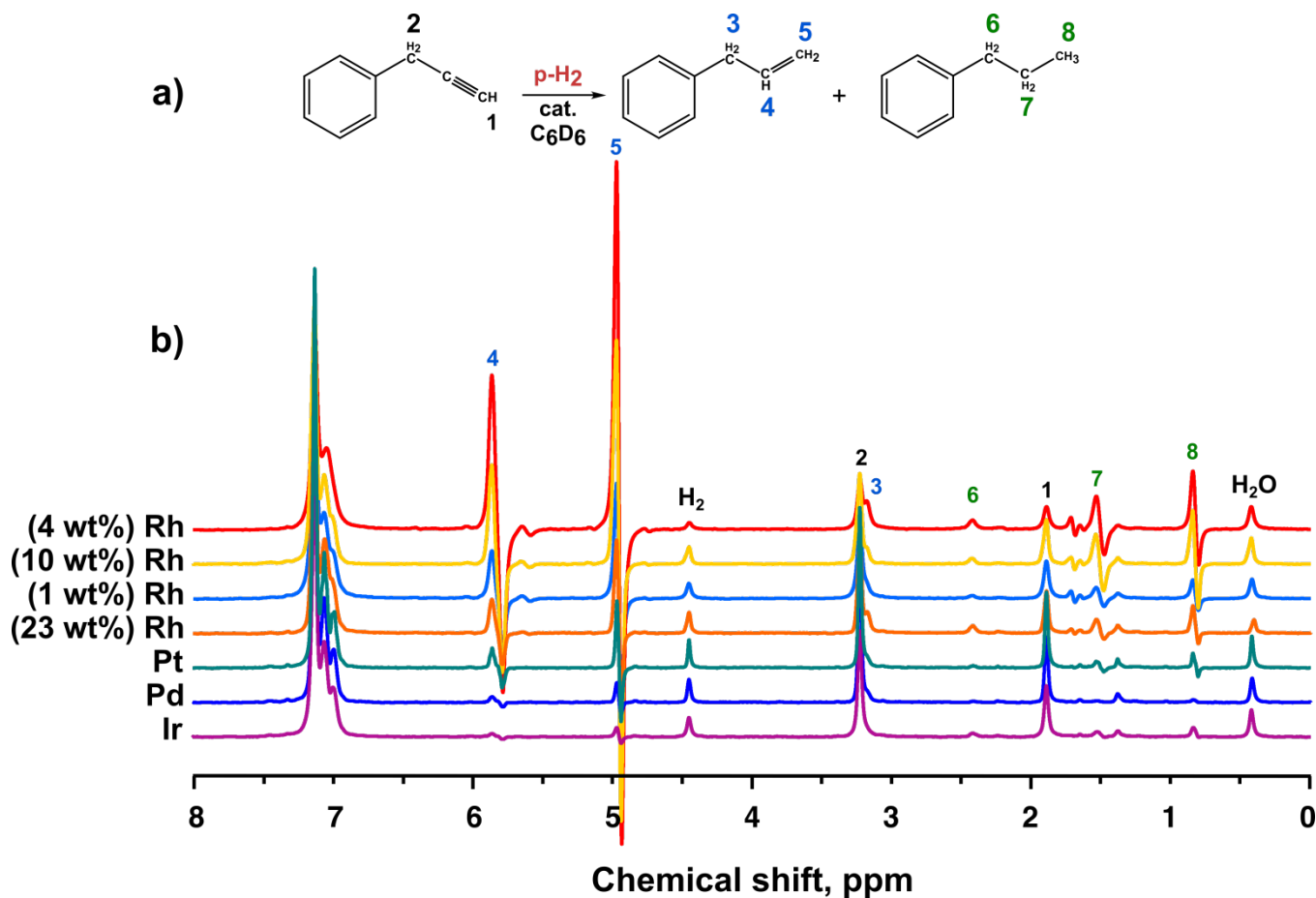


**Figure S6** - (a) Reaction scheme of 3-phenyl-1-propyne hydrogenation. (b)  $^1\text{H}$  NMR spectra acquired during hydrogenation of 3-phenyl-1-propyne with parahydrogen over different heterogeneous catalysts. Spectra are arranged (top to bottom) in descending order of polarized signal intensity (signal #5).

### 3.REPRODUCIBILITY TEST

Two identical experiments with phenylacetylene hydrogenation with parahydrogen over Rh/TiO<sub>2</sub> (10 wt%) were performed. Catalyst sample (10 mg) was placed at the bottom of a 5 mm medium-walled NMR tube and 0.5 mL of a 0.2 M solution of phenylacetylene in benzene-d<sub>6</sub> was added. Parahydrogen was bubbled through the solution at atmospheric pressure for 30 s.  $^1\text{H}$  NMR spectra were acquired immediately after termination of the gas flow.

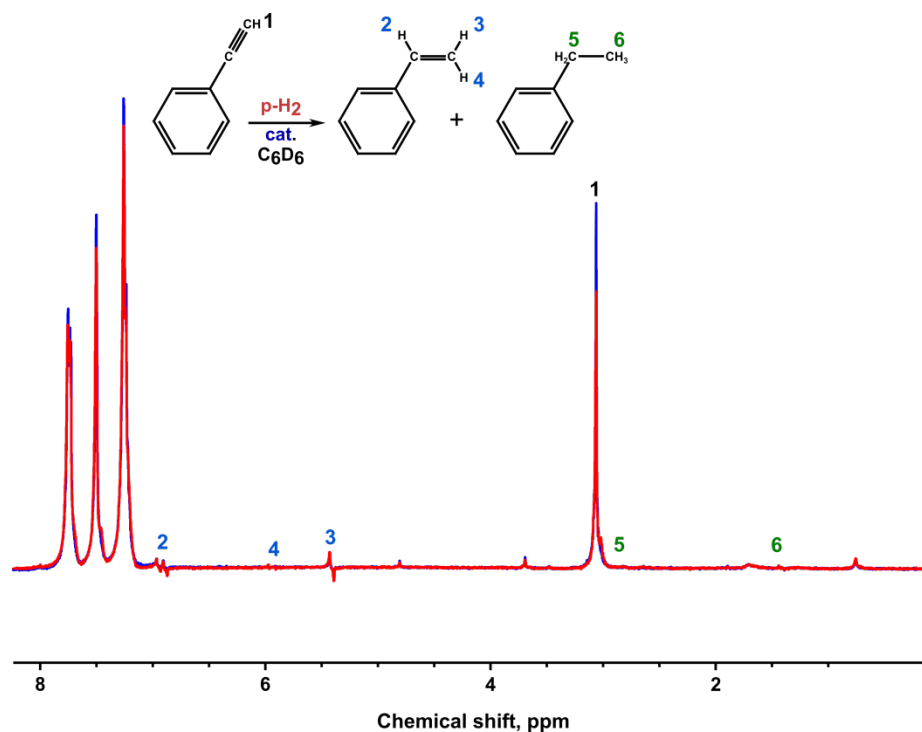


**Figure S7** - PASADENA  $^1\text{H}$  NMR spectra acquired during hydrogenation of phenylacetylene with parahydrogen over 10% Rh/TiO<sub>2</sub>.

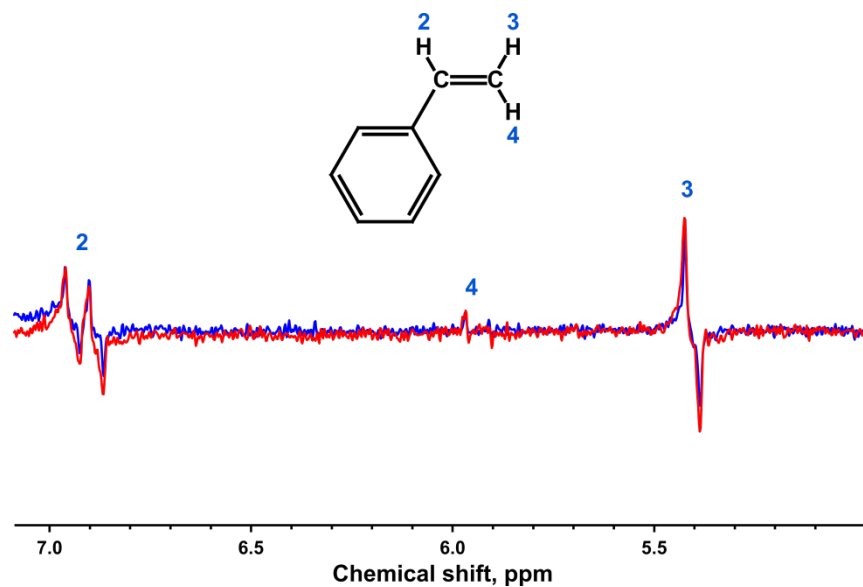


**Figure S8** - Selected regions of spectra from Fig.S7 with signals from styrene protons acquired during hydrogenation of phenylacetylene with parahydrogen over 10% Rh/TiO<sub>2</sub>.

#### 4. OLIGOMERIZATION

In some cases, along with the main hydrogenation reaction, polymerization processes can take place. Table S1 presents indications of oligomerization side process in hydrogenation of all substrates over all catalysts.

**Table S1** - The observation of oligomerization processes in hydrogenation reactions over all catalysts under study.

	Rh (1%)	Rh (4%)	Rh (10%)	Rh (23%)	Pd	Ir	Pt
Phenylacetylene	-	+	+	-	++	-	+
1-phenyl-1-propyne	-	-	-	-	-	-	-
3-phenyl-1-propyne	+	-	+	+	-	-	-

"-" stands for no observation of oligomerization; "+" - observation of oligomerization; "++" - extensive oligomerization.

## 5. STEREOSELECTIVITY

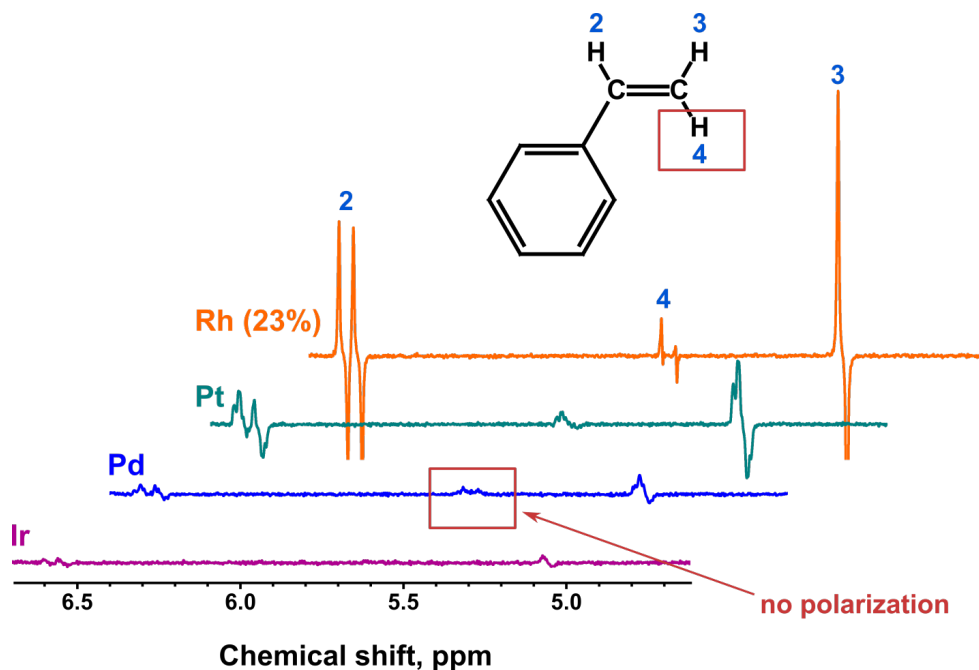


**Figure S9** - A selected region of  $^1\text{H}$  NMR spectra (with signals from styrene protons) acquired during phenylacetylene hydrogenation with parahydrogen over Rh/TiO<sub>2</sub> (23%), Pt/TiO<sub>2</sub>, Pd/TiO<sub>2</sub>, and Ir/TiO<sub>2</sub>. Shown spectra are reprinted from Figure 1 with selected enlarged area with the signals of interest.

Table S2 - Found values of conversion rates and selectivity towards alkene formation in hydrogenation of 1-phenyl-1-propyne and 3-phenyl-1-propyne over all tested catalyst. It should be noted that the selectivity values for phenylacetylene hydrogenation are impossible to calculate due to lack of the signals from thermally polarized products.

Catalyst	1-phenyl-1-propyne hydrogenation		3-phenyl-1-propyne hydrogenation	
	Total conversion, %	Selectivity, %	Total conversion, %	Selectivity, %
Rh (1%)	4	60	21	89
Rh (4%)	56	69	52	80
Rh (10%)	23	39	21	73
Rh (23%)	14	51	34	78

Pd	5	62	8	95
Ir	9	70	14	78
Pt	6	64	7	77

## 6. SOLUBILITY OF HYDROGEN AND HENRY'S LAW

Prior to kinetic experiments it was estimated that 30 seconds of hydrogen bubbling is enough for creating an equilibrium hydrogen concentration in solution, which is defined by Henry's law. In order to understand the applicability of the Henry's law to our experiments, we have measured the concentration of hydrogen in a saturated  $C_6D_6$  solution at different gas pressures. Concentration of hydrogen in benzene at 1atm hydrogen pressure was taken from the Ref. <sup>5</sup>, and concentrations at other pressures were calculated proportionally from the NMR spectra. The obtained results are presented at Figure S10, and it can be seen that generally the data satisfies Henry's law. As a result, we can conclude that hydrogen concentration in the solution is indeed proportional to the hydrogen pressure.

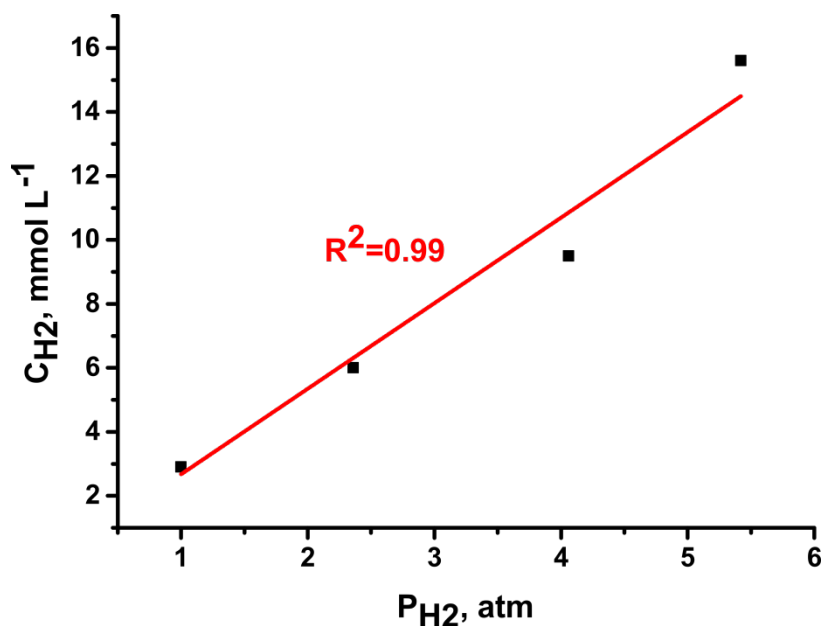


**Figure S10** - Graph of the hydrogen concentration in benzene- $d_6$  solution ( $C_{H_2}$ ) versus hydrogen pressure ( $P_{H_2}$ ).

We have also performed a control experiment in order to make evidence that the hydrogen concentration in solution is stable during the experiment. For this purpose normal hydrogen was bubbled through the acetone- $d_6$  solution (without substrate addition) at 2.7 atm pressure for 30 seconds, then the gas flow was terminated (the total pressure in the system 2/7 atm. was controlled by safety valve) and  $^1H$  NMR spectra were acquired after different time intervals (Fig. S11). The intensities of hydrogen NMR signal were found to be same.

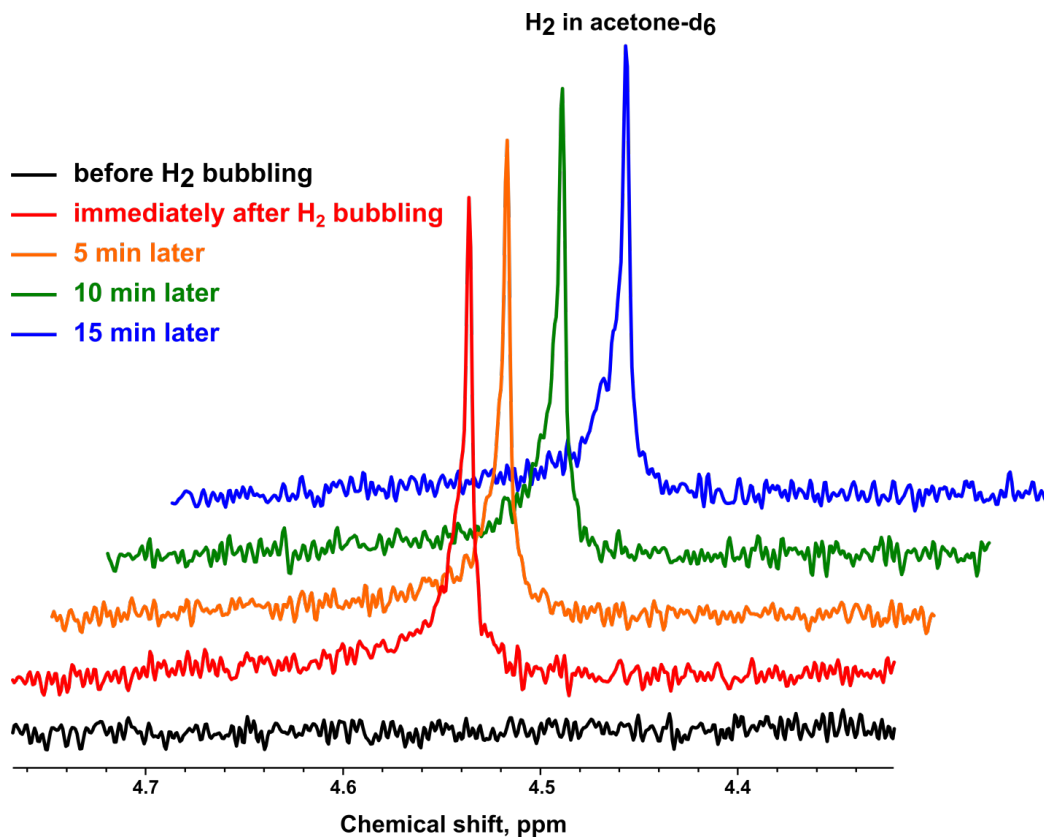
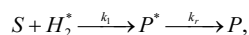


**Figure S11** - A selected region of  $^1H$  NMR spectra (with signals from hydrogen, dissolved in acetone- $d_6$ ) acquired before  $H_2$  bubbling (black line), immediately after  $H_2$  flow termination (red line) and 5, 10 or 15 minutes after  $H_2$  flow termination (orange, green and blue lines, correspondingly).

## 7. KINETIC EXPERIMENTS

The kinetics of the process of pairwise parahydrogen addition, resulting in the formation of hyperpolarized reaction products, can be described by the following simplified model:



where  $S$  is the substrate (here phenylacetylene, 1-phenyl-1-propyne, or 3-phenyl-1-propyne),  $H_2^*$  denotes parahydrogen,  $P^*$  and  $P$  are hyperpolarized and thermally polarized reaction products, respectively,  $k_i$  is the rate constant for the first rate-determining step, and  $k_r$  is the constant for the hyperpolarized product relaxation step (in PASADENA experiments  $k_r$  is equal to  $1/T_1$ , the inverse of the longitudinal spin relaxation time for the hyperpolarized product). The rate of the first step  $W_1$  can be found as:

$$W_1 = k_i [S]^{n_s} [H_2^*]^{n_{H_2^*}},$$

where  $n_s$  and  $n_{H_2^*}$  are the reaction orders with respect to substrate and parahydrogen, respectively. Because of the fast nuclear spin relaxation of the hyperpolarized product and the relatively minor contribution of pairwise hydrogen addition to the overall reaction, it is reasonable to use a steady-state approach for  $[P^*]$ :

$$\frac{d[P^*]}{dt} = W_1 - k_r [P^*] = 0 \Rightarrow [P^*] = \frac{W_1}{k_r} = \frac{k_i [S]^{n_s} [H_2^*]^{n_{H_2^*}}}{k_r}.$$

In the kinetic equation above  $W_1$  quantifies the generation of hyperpolarized product originating from hydrogenation, and the term  $k_r [P^*]$  denotes hyperpolarized product relaxation. As a result, it can be concluded that the concentration of hyperpolarized product  $[P^*]$  (and hence its NMR signal) is proportional to the concentration of parahydrogen (and, thus according to Henry's law, to the parahydrogen pressure  $P_{H_2^*}$  as well; see section 6 in the SI) to the power of  $n_{H_2^*}$ , and thus it is possible to determine the reaction order with respect to parahydrogen for pairwise hydrogen addition by plotting a graph in logarithmic coordinates:  $\ln(\text{PHIP signal})$  versus  $\ln(P_{H_2^*})$ , as shown in Figure S12. It was found that reaction orders are close to unity for all substrates under study.



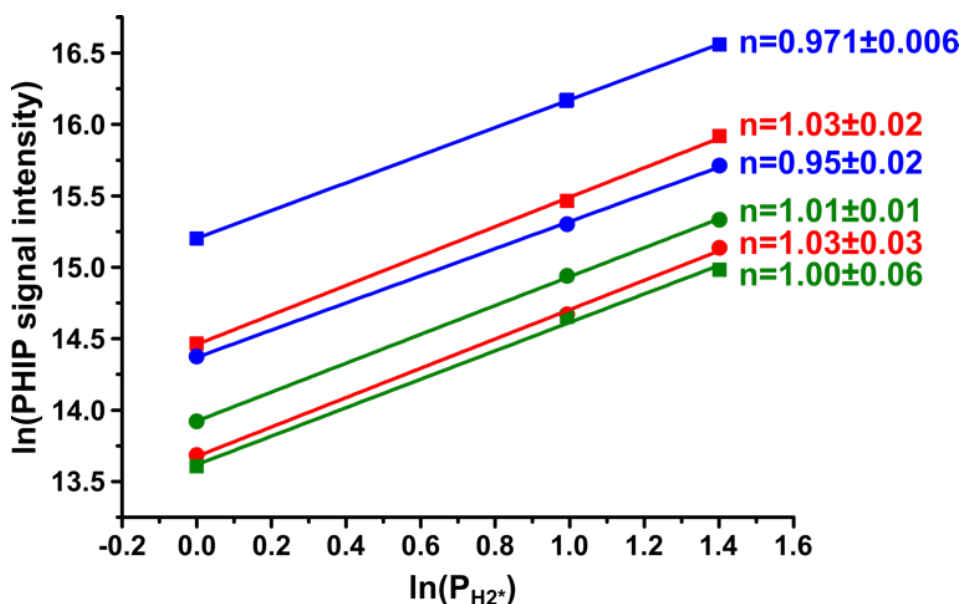


**Figure S12.** Graphs of  $\ln(\text{PHIP signal})$  versus  $\ln(P_{H_2^*})$  for hydrogenation of phenylacetylene, 1-phenyl-1-propyne, and 3-phenyl-1-propyne with parahydrogen; primary products for these reactions are respectively styrene, 1-phenyl-1-propene, and 3-phenyl-1-propene. Red circles: styrene CH-group signal at 6.58 ppm; red squares: styrene proton from CH<sub>2</sub>-group (proton #3 in Fig.1 main text) signal at 5.07 ppm; green circles: 1-phenyl-1-propene CH-group signal at 6.42 ppm; green squares: 1-phenyl-1-propene CH-group signal at 5.63 ppm; blue circles: 3-phenyl-1-propene CH-group signal at 5.84 ppm; blue squares: 3-phenyl-1-propene CH<sub>2</sub>-group signal at 4.97 ppm. The reaction orders estimated from linear fits with respect to parahydrogen are written near each line.

We have also studied kinetics of phenylacetylene hydrogenation with normal hydrogen in order to compare the reaction order with respect to hydrogen for pairwise (hydrogenation with p-H<sub>2</sub>) and non-pairwise (hydrogenation with normal hydrogen, since pairwise addition route is not the main mechanism for overall hydrogenation and thus can be neglected) addition routes. The found reaction order was 0.867, however, since our kinetic experiments were carried out inside the NMR spectrometer, there are some equipment limitations. For instance we cannot provide

shaking of the sample after dissolving normal hydrogen in order to ensure that in the following 10 minutes of kinetic curve registration the reaction proceeds in kinetic mode. In principle, in our setup it is possible that the reaction with normal hydrogen without shaking is being controlled by hydrogen diffusion to the catalyst.<sup>6</sup> On the other hand, the obtained reaction orders are in good agreement with literature data.<sup>7-9</sup> Our observation comes in contrast with previous report for gas-phase hydrogenation of propene over Pt/Al<sub>2</sub>O<sub>3</sub><sup>10</sup>, where reaction orders with respect to hydrogen were vastly different for pairwise and non-pairwise H<sub>2</sub> addition – and this fact emphasize the possible contributions of different mechanisms leading to the pairwise hydrogen addition route on different catalytic systems.

Kinetics studies of liquid-phase hydrogenation over 10 wt% Rh/TiO<sub>2</sub> catalyst with normal hydrogen and parahydrogen were performed in order to estimate the reaction order with respect to hydrogen. For hydrogenation with normal hydrogen (*n*H<sub>2</sub>), the dependence of the ratio of the hydrogen concentration (*C*) at time *t* to the initial hydrogen concentration (*C*<sub>0</sub>) was plotted and fitted with the exponential function:

$$C/C_0 = a \cdot \exp(-t/b) + c, \quad (1)$$

where *a*, *b*, and *c* are fitting parameters. The resulting graph is presented in Figure S13.

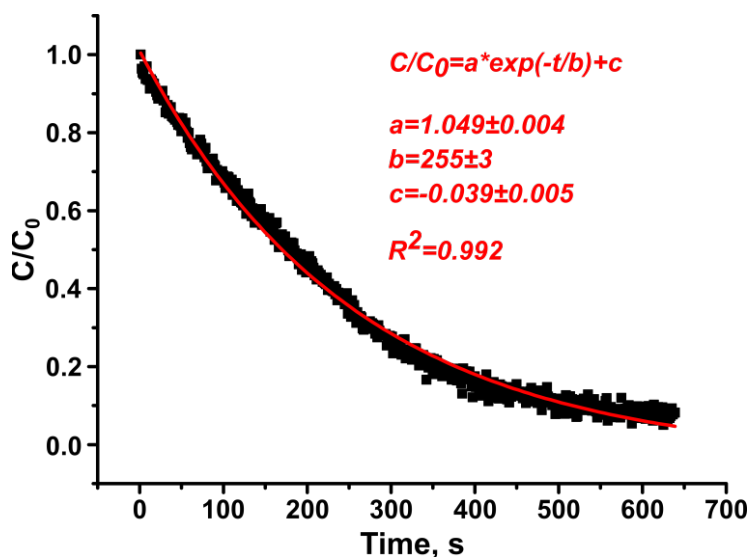


**Figure S13** - Kinetics curve for hydrogenation of phenylacetylene with *n*H<sub>2</sub>. The experimental data points (determined from <sup>1</sup>H NMR) are well-reproduced by a simple exponential fit (red curve).

Next, the reaction rate ( $W$ ) was estimated using a formula obtained by differentiation of the fitting function for concentration (Equation 1) with respect to time:

$$W = -\frac{dC}{dt} = \frac{C_0 \cdot a}{b} \cdot \exp(-t/b),$$

According to the law of mass action,  $W$  is proportional to hydrogen concentration ( $C$ ) to the power of the reaction order with respect to hydrogen ( $n$ ), and, consequently,  $n$  was estimated from a slope of the graph of  $\ln W$  versus  $\ln C$  according to the formula  $\ln W = n \cdot \ln C + \text{const}$  (Figure S14). The resulting overall reaction order for (mostly non-pairwise) hydrogenation was  $0.867 \pm 0.006$ .

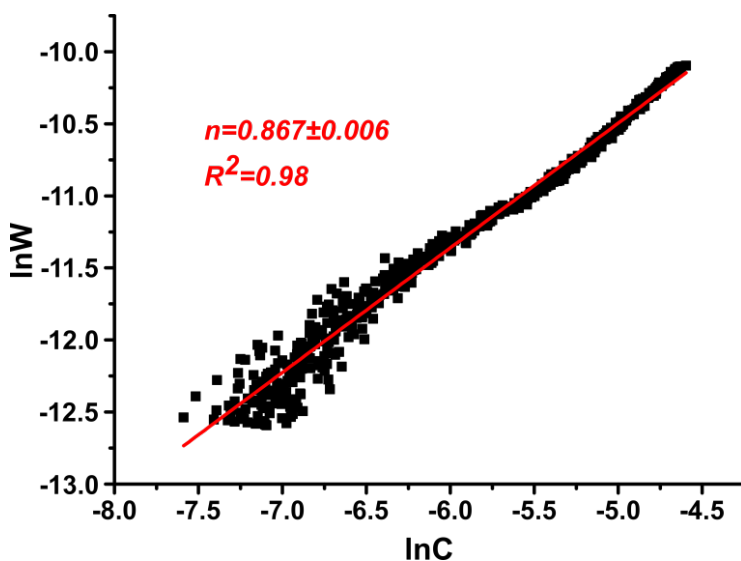


**Figure S14** - Graph of the natural log of the reaction rate ( $\ln W$ ) versus  $\ln C$ , where  $C$  is the time-dependent concentration of hydrogen during hydrogenation of phenylacetylene with normal hydrogen. The slope  $n$  of the linear fit (red line) provides an estimate of the reaction order with respect to hydrogen.

Since our kinetic experiments were carried out inside the NMR spectrometer, there are some equipment limitations – for instance we cannot provide shaking of the sample after dissolving  $n\text{-H}_2$  in order to ensure that in the following 10 minutes of kinetic curve registration the reaction proceeds in kinetic mode. In principle, in our setup it is possible that the reaction with  $n\text{-H}_2$  without shaking is being controlled by hydrogen diffusion to the catalyst.<sup>6</sup> Note that in the kinetic experiments with parahydrogen this is not a problem, since there we acquired the spectra

immediately after stopping the gas flow and didn't register the kinetic curve (the analysis was performed by the signal intensity of the hyperpolarized product).

## REFERENCES

- 1 D. Vasilchenko, S. Vorob'eva, S. Tkachev, I. Baidina, A. Belyaev, S. Korenev, L. Solovyov and A. Vasiliev, Rhodium(III) Speciation in Concentrated Nitric Acid Solutions, *Eur. J. Inorg. Chem.*, 2016, **2016**, 3822–3828.
- 2 D. Dou, D. J. Liu, W. B. Williamson, K. C. Kharas and H. J. Robota, Structure and chemical properties of Pt nitrate and application in three-way automotive emission catalysts, *Appl. Catal. B Environ.*, 2001, **30**, 11–24.
- 3 F. Drault, C. Comminges, F. Can, L. Pirault-Roy, F. Epron and A. Le Valant, Palladium, iridium, and rhodium supported catalysts: Predictive H<sub>2</sub> chemisorption by statistical cuboctahedron clusters model, *Materials (Basel)*, , DOI:10.3390/ma11050819.
- 4 B. J. Kip, F. B. M. Duivenvoorden, D. C. Koningsberger and R. Prins, Determination of metal particle size of highly dispersed Rh, Ir, and Pt catalysts by hydrogen chemisorption and EXAFS, *J. Catal.*, 1987, **105**, 26–38.
- 5 S. Kruyer and A. P. P. Nobel, Solubility of hydrogen in benzene, cyclohexane, decalin, phenol and cyclohexanol, *Recl. des Trav. Chim. des Pays-Bas*, 1961, **80**, 1145–1156.
- 6 B. E. Shutt and J. M. Winterbottom, Heterogeneous Catalysis in the Liquid Phase, *Platin. Met. Rev.*, 1971, **15**, 94–99.
- 7 B. A. Wilhite, A. M. J. McCready and A. Varma, Kinetics of Phenylacetylene Hydrogenation over Pt/ $\gamma$ -Al<sub>2</sub>O<sub>3</sub> Catalyst, *Ind. Eng. Chem. Res.*, 2002, **41**, 3345–3350.
- 8 J.-L. Pellegatta, C. Blandy, V. Collière, R. Choukroun, B. Chaudret, P. Cheng and K. Philippot, Catalytic investigation of rhodium nanoparticles in hydrogenation of benzene and phenylacetylene, *J. Mol. Catal. A Chem.*, 2002, **178**, 55–61.
- 9 U. Syunbayev, D. K. Churina, G. Y. Yergaziyeva, N. A. Assanov and K. K. Kalihanov, The Liquid-Phase Hydrogenation of Citral to Citronellal at Hydrogen Pressure, *Int. J.*

*Chem. Eng. Appl.*, 2016, **7**, 133–137.

- 10 O. G. Salnikov, K. V. Kovtunov, D. A. Barskiy, V. I. Bukhtiyarov, R. Kaptein and I. V. Koptug, Kinetic Study of Propylene Hydrogenation over Pt/Al<sub>2</sub>O<sub>3</sub> by Parahydrogen-Induced Polarization, *Appl. Magn. Reson.*, 2013, **44**, 279–288.